Bioorganic & Medicinal Chemistry Letters 19 (2009) 6557–6560

Contents lists available at ScienceDirect

Bioorganic & Medicinal Chemistry Letters

journal homepage: www.elsevier.com/locate/bmcl

Structural basis for the inhibitor recognition of human Lyn kinase domain

Nao Miyano [a], Takayoshi Kinoshita [a], Ryoko Nakai [b], Yasuyuki Kirii [b], Koichi Yokota [b], Toshiji Tada [a,*]

[a] Graduate School of Science, Osaka Prefecture University, 1-1 Gakuen-cho, Naka-ku, Sakai, Osaka 599-8531, Japan
[b] Carna Biosciences, Inc., 3rd Floor, BMA, 1-1-5 Minatojima-Minamimachi, Chuo-ku, Kobe, Hyogo 650-0047, Japan

ARTICLE INFO

Article history:
Received 14 July 2009
Revised 4 October 2009
Accepted 8 October 2009
Available online 13 October 2009

Keywords:
Lyn
Src family
Kinase
Structure
Inhibitor

ABSTRACT

Human Lyn tyrosine kinase is expressed in hematopoietic tissues and plays crucial roles in the signal transduction of hematopoietic immune system. Its excess activity is involved in several tumors. The crystal structure has revealed that the potent inhibitor staurosporine binds to human Lyn kinase domain at the ATP-binding site. The remarkable structural features of the staurosporine-binding region will offer valuable structural insights for the structure-based design of novel Lyn-selective inhibitors.

Src family protein tyrosine kinases (SFKs) comprise of Src, Lyn, Fyn, Yes, Lck, Hck, Fgr, Blk and Frk. All of these kinases are about 60 kDa in molecular weight and possess the high homologies of the amino acid sequences. They have a common structure consisting of an N-terminal unique sequence and SH3, SH2, and kinase (SH1) domains followed by a C-terminal regulatory tail.[1] SFKs have been implicated in signaling pathways that control many different cellular functions, including immune cell activation, cell growth, differentiation, survival, adhesion, and migration.[2,3] Abnormal SFK signaling has been linked to several disease states, involving osteoporosis and cancer metastases.[4]

Lyn is widely expressed in B lymphocytes and myeloid cells. Lyn established thresholds by acting as both a positive and a negative modulator of a variety of signaling responses.[5,6] Lyn deficiency in mice causes a loss of inhibitory signaling, resulting in autoimmunity, renal disease and premature mortality. Interestingly, the same phenotype is produced by the hyperactive Lyn in mice.[7–9] These results clearly show that the balance of Lyn signaling, in either a positive sense or an inhibitory sense is important. However, the overall role of Lyn as a modulator in the signal transduction of immune system is much less well understood. Lyn-selective inhibitor will be useful to elucidate how Lyn regulates signaling thresholds within B lymphocytes and myeloid cells. Lyn is an important candidate target for specific therapy of prostate cancer,[10] colon cancer[11,12] and acute myeloid leukemia.[13,14] Furthermore, recent studies show that activation of Lyn is associated with resistance to imatinib, which is the standard therapy for newly diagnosed chronic myelogenous leukemia.[15]

Lyn inhibitors have potency as the anti-allergic drug and/or the anti-cancer drug. The selective inhibitor for Lyn would recover the Lyn-driven disorders without serious side effects occurred by the inhibition of other kinases. However, no potent Lyn-selective inhibitor has been reported nowadays. Here, we report the crystal structure[16] of Lyn kinase domain complexed with staurosporine (Fig. 1), which is a prototypical ATP-competitive kinase inhibitor in that it binds to many kinases with high affinity. A detailed comparison of the crystal structure of Lyn-staurosporine complex with those of the Fyn-staurosporine complex[17] and the Lck-staurosporine complex[18] confers clues to production of Lyn inhibitors with high selectivity over the other Src family kinases.

Overall structure is shown in Figure 2. The nine amino acid residues 392–400, referred to as the activation loop (A-loop) were disordered and did not show clear electron densities for assignment, possibly because the A-loop is flexible. Activity assay and western blot analysis showed that the recombinant Lyn had unphosphorylated Tyr396 and was inactive form. Generally, inactive Lyn, in which Tyr396 is unphosphorylated, has a flexible A-loop.[19]

The clear electronic density map corresponding to staurosporine molecule was found at the ATP-binding site located between the N- and C-lobes of Lyn kinase domain (Fig. 3). The staurosporine molecule binds to Lyn by three hydrogen bonds, a CH–O interaction, and eight CH-π type interactions. The NH group and carbonyl oxygen of the lactam ring of the inhibitor made a pair of hydrogen bonds with the backbone carbonyl oxygen of Glu320 and the backbone NH of Met322. Both amino acid residues in the hinge region are important for binding of the adenine ring of ATP

* Corresponding author. Tel.: +81 72 254 9820; fax: +81 72 254 9935.
E-mail address: tada@b.s.osakafu-u.ac.jp (T. Tada).

0960-894X/$ - see front matter © 2009 Elsevier Ltd. All rights reserved.
doi:10.1016/j.bmcl.2009.10.038

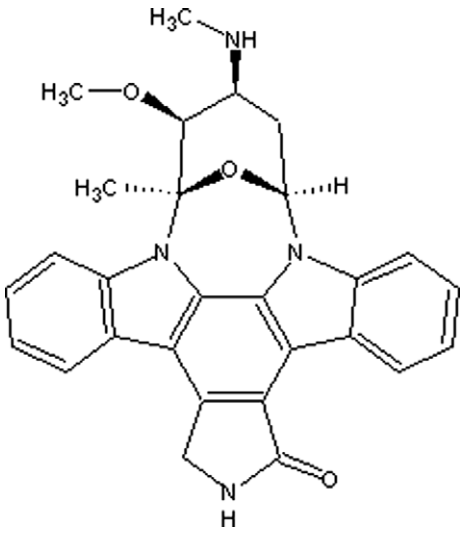

Figure 1. Chemical structure of staurosporine.

to protein kinases. The methylamino nitrogen of the glycosidic ring formed a hydrogen bond to the backbone carbonyl oxygen of Ala371 in the ribose-binding pocket of Lyn. The glycosidic oxygen of staurosporine participated in a CH–O interaction with the backbone C_α atom of Gly254. The CH–O interaction is well defined in small-molecule crystal structures[20] and has also been observed in other kinases.[17,18] The plane structure moiety of staurosporine molecule was surrounded by the five hydrophobic residues, including Leu253, Val261, and Ala273 from the N-lobe, and Gly325 and Leu374 from the C-lobe. A total of eight CH groups from these residues interacted with the conjugated plane of the inhibitor. All interactions were conserved in the Fyn- and Lck-staurosporine complexes. These common structural features coincided with analogous inhibitory activities of staurosporine for Lyn, Fyn and Lck (Table 1). Structural differences around the staurosporine-binding region appeared to drive selectivity for each kinase (Fig. 4).

A notable sequence difference among the three kinases, Lyn, Lck and Fyn was found at the glycine-rich loop (G-loop) covered the edge of the ATP-binding site. The amino acid sequence of the G-loop of Lyn is GAGQFG and is identical with that of Lck, while

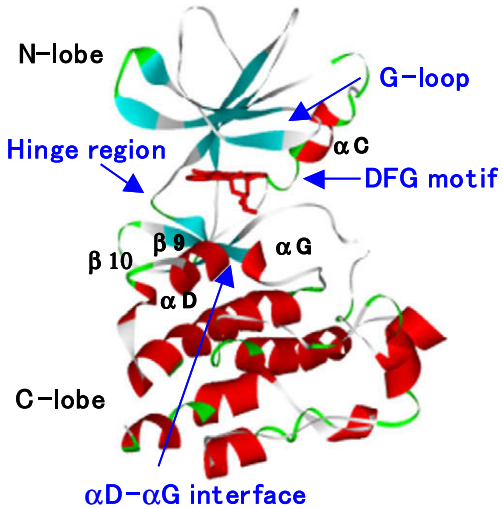

Figure 2. Overall structure of the Lyn-staurosporine complex. Staurosporine binds to the ATP-binding site which is located at the large groove between the N- and C-lobes united by the hinge region.

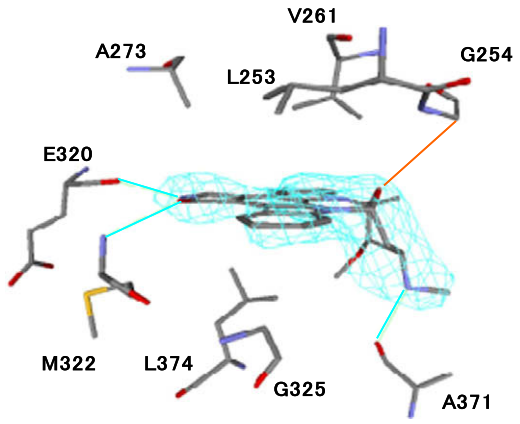

Figure 3. Fo–Fc map at 1.5σ level around the staurosporine. Selected amino acid residues are drawn. Hydrogen bonds and CH–O interaction are shown by blue and orange lines, respectively.

Table 1
The inhibition of protein tyrosine kinases by staurosporine

	Lyn	Fyn	Lck
IC_{50} (nM)	1.3	2.0	1.5

the alanine residue is replaced with the asparagines residue in Fyn (Fig. 4A). The asparagine residue has a relatively rigid conformation due to the formation of a hydrogen bond with Glu260 (Lyn numbering scheme) which is conserved in the three kinases. Thus, the carbonyl oxygen atom of the asparagine residue is fixed toward the ATP-binding site and has potency to make an interaction with inhibitor molecules.

A characteristic groove is formed between two α-helices, αD and αG. Lyn and Fyn have relatively narrow and shallow grooves, because hydrogen bonds are formed between the NH of Leu328 of αD helix and carbonyl of Ala370 of αG helix in Lyn and between the NH of Leu350 of αD and the hydroxyl and/or carbonyl of Ser392 of αG in Fyn (Fig. 4B). On the other hand, Lck has Val325 at the same position of αD helix. The Val325 residue will disturb the formation of the short contact between αD and αG helices because of the steric hindrance between the $C_{\gamma1}$ atom of Val325 and Ala367 residues of αG helix. This suggests that relatively large inhibitor molecules might be held in the groove of Lck which is slightly large and deep in comparison with those of Lyn and Fyn.[21]

Lyn has Ala323 at the hinge region, whereas Fyn and Lck have Asn345 and Glu320, respectively (Fig. 4C). The alanine residue has a small side chain compared with the asparagine and glutamic acid residues. Thus, a cavity was generated around the hinge region of Lyn. The cavity will be useful for the molecular design of novel Lyn-selective inhibitors. The position of the turn structure between β-strands 9 and 10 was shifted toward the N-lobe. This seems to be caused by an electrostatic interaction between Glu377 of the turn structure and Lys271 of the N-lobe. As a result, Glu377 approaches Ala323. Thus, the negative charge will also be useful for the Lyn-selective inhibitor design, such as the addition of dimethylaminopropyl pyridine. The moiety could use the features of the relatively large cavity and the negatively charged Glu377 effectively.[22]

The DFG motif at the beginning of A-loop is the key structural component of active kinases. The DFG motif has the 'DFG-In' conformation in the active state and is flipped into its inactive 'DFG-Out' conformation. In the structure of Lyn complexed with staurosporine, the DFG motif has the 'DFG-In' conformation. Staurosporine is the Type I kinase inhibitor that does not require the DFG motif in its inactive 'DFG-Out' conformation.[23] Interestingly,

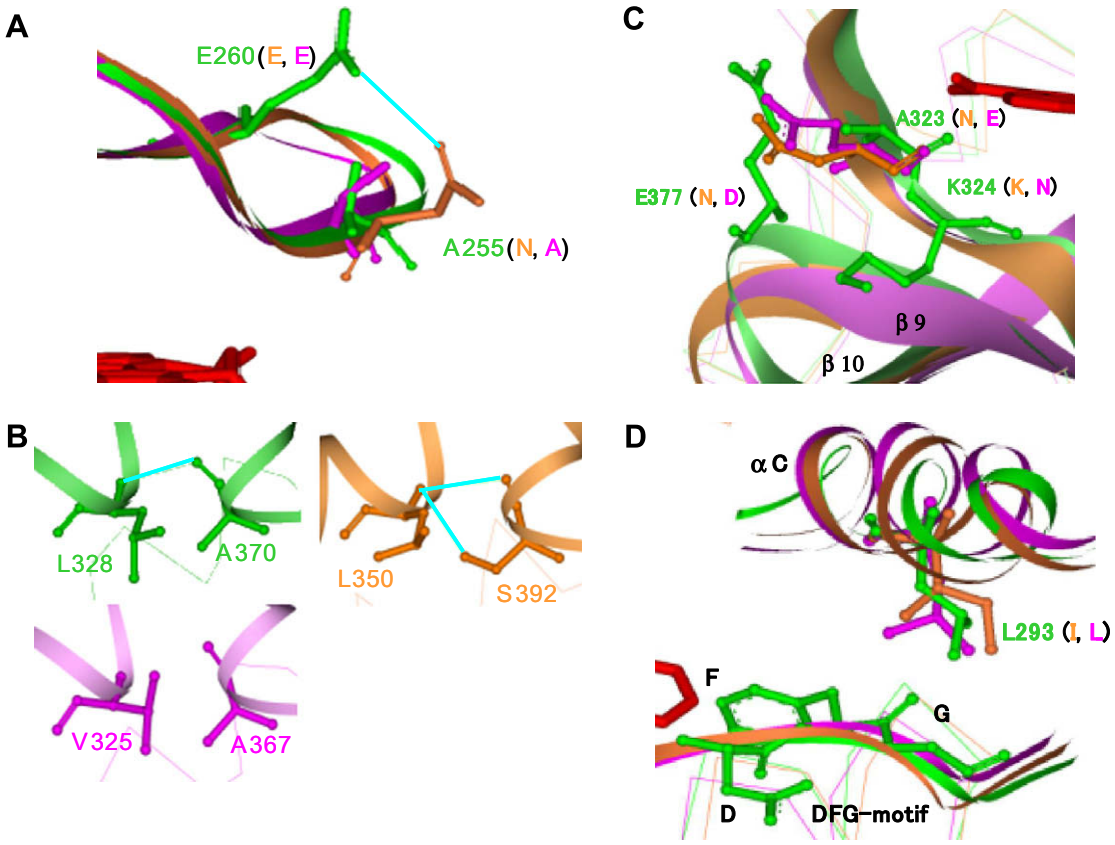

Figure 4. Superimposition of Lyn- (green), Fyn- (orange), and Lck- (pink) Staurosporine complex structure. The hydrogen bonds are shown by blue line. (A) G-loop. (B) αD and αG helices. (C) Hinge region. (D) DFG motif.

Fyn has the isoleucine residue at the αC helix which is near the glycine residue of the DFG motif, whereas Lyn and Lck have the leucine residue (Fig. 4D). This suggests that Fyn induces a slightly larger cavity between the DFG motif and αC helix than Lyn and Lck, when the three kinases have the 'DFG-Out' conformation. Imatinib, which is the Type II and the selective inhibitor for Abl kinase, has been reported to bind Abl in the "DFG-Out" conformation.[24] Thus, it is available to utilize the cavity for the design of Fyn-selective inhibitors.

In conclusion, we determined the crystal structure of human Lyn kinase domain complexed with staurosporine. The cavity generated around the hinge region and the negative charged Glu377 of Lyn will be useful for the creation of the novel inhibitor which has high affinity and selectivity to Lyn. Although the high affinity should be compensated by attractive interactions, the selectivity of inhibitor for a specific target enzyme can be obtained also by using the effect of the steric repulsions. The structural features of Lyn-, Fyn- and Lck-staurosporine complexes also suggest that the affinity of inhibitor for Fyn and Lyn will be reduced relative to Lck by the steric repulsions with the carbonyl of the asparagine residue of the G-loop and with the characteristic groove formed between two α-helices, αD and αG. These remarkable structural features of the staurosporine-binding region will offer valuable structural insights for the structure-based design of novel Lyn-selective inhibitors.

Acknowledgments

The synchrotron radiation experiments were done at Photon Factory with the approval of the Japan Synchrotron Radiation Research Institute. We thank the staff for their help in data collection at the NW-12 station.

References and notes

1. Lowell, C. A. *Mol. Immunol.* **2004**, *41*, 631.
2. Thomas, S. M.; Brugge, J. S. *Annu. Rev. Cell Dev. Biol.* **1997**, *13*, 513.
3. Okutani, D.; Lodyga, M.; Han, B.; Liu, M. *Am. J. Physiol. Lung Cell Mol. Physiol.* **2006**, *291*, 129.
4. Summy, J. M.; Gallick, G. E. *Cancer Metastasis Rev.* **2003**, *22*, 337.
5. Chan, V. W. F.; Meng, F.; Soriano, P.; DeFrance, A. L.; Lowell, C. A. *Immunity* **1997**, *7*, 69–81.
6. Janas, M. L.; Hodgkin, P.; Hibbs, M.; Tarlinton, D. *J. Immunol.* **1999**, *163*, 4192.
7. Harder, K. W.; Parsons, L. M.; Armes, J.; Evans, N.; Kountouri, N.; Clark, R.; Quilici, C.; Grail, D.; Hodgson, G. S.; Dunn, A. R.; Hibbs, M. L. *Immunity* **2001**, *15*, 603.
8. Hibbs, M. L.; Harder, K. W.; Armes, J.; Kountouri, N.; Quilici, C.; Casagranda, F.; Dunn, A. R.; Tarlinton, D. M. *J. Exp. Med.* **2002**, *196*, 1593.
9. Xiao, W.; Nishimoto, H.; Hong, H.; Kitaura, J.; Nunomura, S.; Maeda-Yamamoto, M.; kawakami, Y.; Lowell, C. A.; Ra, C.; Kawakami, T. *J. Immunol.* **2005**, *175*, 6885.
10. Goldenberg-Furmanov, M.; Stein, I.; Pikarsky, E.; Rubin, H.; Kasem, S.; Wygoda, M.; Weinstein, I.; Reuveni, H.; Ben-Sasson, S. A. *Cancer Res.* **2004**, *64*, 1058.
11. Bates, R. C.; Edwards, N. S.; Burns, G. F.; Fisher, D. E. *Cancer Res.* **2001**, *61*, 5275.
12. Subramaniam, V.; Vincent, I. R.; Gardner, H.; Chan, E.; Dhamko, H.; Jothy, S. *Exp. Mol. Path.* **2007**, *83*, 207.
13. Roginskaya, V.; Zuo, S.; Caudell, E.; Nambudiri, G.; Kraker, A. J.; Corey, S. J. *Leukaemia* **1999**, *13*, 855.
14. Okamoto, M.; Hayakawa, F.; Miyata, Y.; Watamoto, K.; Emi, N.; Abe, A.; Kiyoi, H.; Towatari, M.; Naoe, T. *Leukemia* **2007**, *21*, 403.
15. Wu, J.; Meng, F.; Kong, L.-Y.; Peng, Z.; Ying, Y.; Bornmann, W. G.; Darnay, B. G.; Lamothe, B.; Sun, H.; Talpaz, M.; Donato, N. J. *J. Nat. Cancer Inst.* **2008**, *100*, 926.
16. Kinoshita, T.; Miyano, N.; Nakai, R.; Yokota, K.; Ishiguro, H.; Tada, T. *Protein Express. Purif.* **2008**, *58*, 318. In order to prepare the inhibitor-Lyn complex, powdered staurosporine was suspended in the concentrated protein solution. After spinning down undissolved inhibitor, crystallization trials were performed by sitting-drop vapor diffusion method at 4 °C. The Lyn-staurosporine complex solution was mixed with an equal volume of a reservoir solution containing 0.2 M NaCl, 25% PEG 3350 and 0.1 M Tris–HCl (pH 8.5) as reported before.[16] Crystals were protected in Paratone-N oil (Hampton Research) as a cryoprotectant before flash freezing in nitrogen-gas stream at 100 K. Diffraction data were collected at a wavelength of 1.00 Å using the synchrotron radiation at Photon Factory beamline NW12A and a CCD detector Quantum 210 (ADSC) with an exposure time of 30 s per image at a crystal to detector distance of 280 mm. X-ray diffraction data consisting of the

139 images were processed and scaled using the program HKL2000. The structure of the complex was solved using the program MolRep in the CCP4 suite. A starting model which was obtained by homology modeling from the Fyn structure, and model building and map fitting were performed using the program DS Modeling (Accelrys). Further refinement involved iterative manual rebuilding and maximum-likelihood refinement using the program CNX. Final refinement was converged to R = 29.3% and R_{free} = 32.4% Final coordinates were deposited to Protein Data Bank (code: 3A4O)..

17. Kinoshita, T.; Matsubara, M.; Ishiguro, H.; Okita, K.; Tada, T. *Biochem. Biophys. Res. Commun.* **2006**, *346*, 840.
18. Zhu, X.; Kim, J. L.; Newcomb, J. R.; Rose, P. E.; Stover, D. R.; Toledo, L. M.; Zhao, H.; Morgenstern, K. A. *Structure* **1999**, *7*, 651.
19. Breitenlechner, C. B.; Kairies, N. A.; Honold, K.; Scheiblich, S.; Koll, H.; Greiter, E.; Koch, S.; Schäfer, W.; Huber, R.; Engh, R. A. *J. Mol. Biol.* **2005**, *353*, 222.
20. Kuduva, S. S.; Craig, D. C.; Nangia, A.; Desiraju, G. R. *J. Am. Chem. Soc.* **1999**, *121*, 1936.
21. There is a report which shows the importance of this groove to the selectivity. See: Burchat, A.; Borhani, D. W.; Calderwood, D. J.; Hirst, G. C.; Li, B.; Stachlewitz, R. F. *Bioorg. Med. Chem. Lett.* **2005**, *16*, 118.
22. A similar molecule design has been reported with the c-Jun N-terminal kinase-3. See: Swahn, B.-M.; Huerta, F.; Kallin, E.; Malmström, J.; Weigelt, T.; Viklund, J.; Womack, P.; Xue, Y.; Öhberg, L. *Bioorg. Med. Chem. Lett.* **2005**, *15*, 5095.
23. Liu, Y.; Gray, N. S. *Nat. Chem. Biol.* **2006**, *2*, 358.
24. Nagar, B.; Bornmann, W. G.; Pellicena, P.; Schindler, T.; Veach, D. R.; Todd Miller, W.; Clarkson, B.; Kuriyan, J. *Cancer Res.* **2002**, *62*, 4236.